PROCEEDINGS OF SCIENCE

Intra-taste eigenvalue splittings of staggered, Karsten-Wilczek and Boriçi-Creutz fermions in 2D

Maximilian Ammer[a] **and Stephan Dürr**[a,b,*]

[a] *Physics Department, University of Wuppertal, D-42119 Wuppertal, Germany*
[b] *IAS/JSC, Forschungszentrum Jülich, D-52425 Jülich, Germany*

E-mail: ammer (AT) uni-wuppertal.de, duerr (AT) uni-wuppertal.de

Staggered, Karsten-Wilczek (KW) and Boriçi-Creutz (BC) fermions all retain a remnant chiral symmetry. The price to be payed is that they are doubled, and the resulting taste symmetry is broken by cut-off effects. We measure the size of the taste symmetry violation by determining the low-lying eigenvalues of these fermion operators in the two-dimensional Schwinger model which admits, like QCD, a global topological charge $q \in \mathbb{Z}$ of a given gauge configuration. We find that it matters whether the pertinent eigenmode is a would-be zero mode or a non-topological mode. The intra-taste splittings of these fermion formulations are all found to diminish with increasing β. Our goal is to verify standard Symanzik scaling for these taste-breaking effects.

The 39th International Symposium on Lattice Field Theory,
8th-13th August, 2022,
Rheinische Friedrich-Wilhelms-Universität Bonn, Germany

* Speaker

1. Introduction

For lattice fermions exact chiral symmetry comes at a price. One option is to start with an undoubled formulation, e.g. the Wilson fermion Dirac matrix $D_{\rm W}$ [1], and to mitigate the effects of additive mass renormalization and operator mixing. Another option is to stay within the category of ultralocal chiral actions, and to live with the fact that an even number of species is encoded.

For a long time, the second category was sparsely populated. Only naive [2] and Susskind ("staggered") fermions [3] with 16 and 4 species, respectively, in four space-time dimensions ("4D") were widely known. More recently, this category has been augmented by Karsten-Wilczek [4, 5] and Boriçi-Creutz fermions [6, 7]. The latter two actions encode only 2 species in 4D, and thus seem attractive for simulating 2-flavor QCD in the isospin limit $m_u^{\rm ren} = m_d^{\rm ren} > 0$.

The two species encoded by one Karsten-Wilczek matrix $D_{\rm KW}$ or one Boriçi-Creutz matrix $D_{\rm BC}$ are referred to as "tastes", to be distinguished from the standard concept of "flavor" [associated with different fields of one action]. The reason is that taste-symmetry is broken by cut-off effects, while flavor symmetry is exact (at finite lattice spacing $a > 0$). In order to simulate QCD with 2 degenerate flavors, one may thus use a single copy of $D_{\rm KW}$ or $D_{\rm BC}$, but one *must take the continuum limit*, since the two species mix at any $a > 0$ in a complicated (a-dependent) fashion.

For staggered fermions there is a long tradition of examining in detail how this taste symmetry breaking (which depends on the specifics how tastes are identified at $a > 0$) disappears under $a \to 0$, see e.g. the MILC paper [8] for a guide to the literature. For Karsten-Wilczek and Boriçi-Creutz fermions we are unaware of similar practical efforts. This is why we feel it is rewarding to take a look at "taste symmetry restoration" (at asymptotically small lattice spacings) for these formulations.

We will examine the situation in the quenched Schwinger model [9, 10] in two space-time dimensions ("2D"). In this case even staggered fermions are "minimally doubled", hence featuring 2 tastes. In our view, this provides an excellent opportunity to compare three 2-species formulations on equal footing. To avoid the need of specifying any taste identification details, we investigate the eigenvalue splittings of these operators. In 2D eigenvalues come in *pairs* for all three formulations (in 4D it would be *quartets* for staggered fermions [11, 12]), and our goal is to demonstrate, for each formulation, a Symanzik-type scaling of the intra-pair splitting of the eigenvalues.

2. Schwinger model: instanton hit updates

We use the action density $s_{\rm wil}(x) = 1 - {\rm Re}(U_\Box(x)) = 1 - \cos(\theta(x))$ for the gauge boson, where the plaquette variable at position $x = (x_1, x_2)$ is $U_\Box(x) = U_1(x)U_2(x+e_1)U_1^\dagger(x+e_2)U_2^\dagger(x) = \exp({\rm i}\theta(x))$. Next, one defines two discretizations of the global topological charge, $q_{\rm raw}^{(n)} = \frac{1}{2\pi}\sum \sin(\theta^{(n)}(x)) \in \mathbb{R}$ and $q_{\rm geo}^{(n)} = \frac{1}{2\pi}\sum \theta^{(n)}(x) \in \mathbb{Z}$, where the sum is over all sites x, and $\theta^{(n)}$ is the plaquette angle after n steps of stout smearing [13]. In the following we shall use $n = 0, 1$ or 3 steps with $\rho = 0.25$ fixed. The "geometric" charge $q_{\rm geo}$ is integer-valued, while the "field-theoretic" charge follows from the "raw" charge through a (β-dependent but finite) renormalization factor, i.e. $q_{\rm fth}^{(n)} = Z^{(n)}(\beta)\, q_{\rm raw}^{(n)}$.

The pure gauge part of the Schwinger model can be simulated by means of a mixture of (multi-hit) Metropolis and overrelaxation sweeps. A striking similarity of this model with pure Yang-Mills theory is that the partition function in the continuum decays into contributions from various topological sectors, i.e. $Z = \sum_{q\in\mathbb{Z}} Z_q$. For $\beta > 6$ the lattice theory (where Z is simply

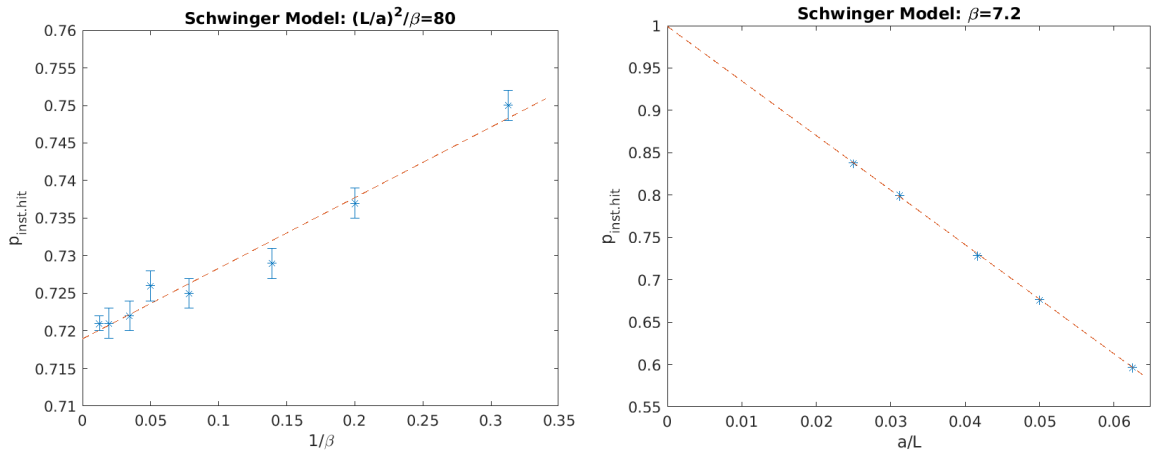

Fig. 1: Instanton hit acceptance ratio $p_{\text{inst.hit}}$ versus $1/\beta$ in a fixed physical volume (left, see Tab. 1), and versus a/L at fixed β (right, see Tab. 2), along with linear fits. Note the different y-ranges.

connected) feels this indirectly, since $Z(\beta)$ gradually consists of big "basins" (where q is reasonably well defined) which are connected by thin "bridges" (where q is not well defined, i.e. different discretizations tend to give rather different results). In the limit $\beta \to \infty$ (or $a \to 0$) the "bridges" evolve into sets of measure zero in configuration space. This sounds good in the sense that $q[U]$ becomes well defined for any typical gauge background U in Z. But it is bad in practical terms, since any update algorithm which evolves U in small steps becomes stuck in a particular topological sector, and thus non-ergodic. This phenomenon is referred to as "topological freezing".

Fortunately, in the quenched Schwinger model the problem has been solved long ago by "instanton hits" (originally in [14], more details are found e.g. in [15]). The idea is to propose update steps which "tunnel through the barrier" between topological sectors, and the respective acceptance rate is found to be large and to tend to 1 in the infinite-volume limit, see Fig. 1.

3. Schwinger model: ensemble details and topological charge distributions

In the Schwinger model the lattice spacing a is conveniently set through the inverse of the (dimensionful) electric charge via $\beta = 1/(ae)^2$. This makes it easy to define, from the beginning, matched ensembles, that is lattices with fixed box size L in physical units. Our 24 main ensembles are generated in this way, see Tab. 1. For each $(\beta, L/a)$ combination three ensembles of 10 000 configurations each are generated. On the first ensemble the low-lying eigenvalues of D_{S}, D_{KW}, D_{BC} are evaluated without link smearing, on the second one after 1 stout step, and on the last one after 3 steps. Tab. 2 lists four extra ensembles to test for finite volume effects.

In each ensemble the plaquette is checked using the analytic result of Ref. [16]. Due to the large acceptance ratio of the instanton-hit proposal (cf. Fig. 1), the topological charges of successive configurations are well decorrelated. As a result, the overall topological charge distribution looks "healthy", regardless whether $q^{(n)}_{\text{geo}}$ or $q^{(n)}_{\text{fth}}$ is used, and regardless of $n \in \{0, 1, 3\}$. Incidentally, for the higher β-values the two definitions of the topological charge agree on all 10'000 configurations in a given ensemble, even in the unsmeared case ($n = n_{\text{stout}} = 0$), see Fig. 2 for an illustration.

β	3.2	5.0	7.2	12.8	20.0	28.8	51.2	80.0
L/a	16	20	24	32	40	48	64	80
n_{stout}	0,1,3	0,1,3	0,1,3	0,1,3	0,1,3	0,1,3	0,1,3	0,1,3
$p_{\text{inst.hit}}$	0.750(2)	0.737(2)	0.729(2)	0.725(2)	0.726(2)	0.722(2)	0.721(2)	0.721(1)

Tab. 1: Overview of the ensembles used in the "cut-off effect" study, implementing constant physical volume through $(L/a)^2/\beta = 80$. For every choice of $(\beta, L/a)$ three ensembles of 10 000 configurations are generated, to be used with 0, 1 or 3 steps of $\rho = 0.25$ stout smearing, respectively.

β	7.2	7.2	7.2	7.2	7.2
L/a	16	20	24	32	40
n_{stout}	1	1	1	1	1
$p_{\text{inst.hit}}$	0.597(2)	0.677(2)	0.729(2)	0.799(2)	0.838(2)

Tab. 2: Overview of the ensembles used in the "finite volume" study at fixed lattice spacing ($\beta = 7.2$). Each ensemble of 10 000 configurations and is used after 1 step of $\rho = 0.25$ stout smearing. In addition, the acceptance ratio of the instanton hit update (see text) at the respective $(\beta, L/a)$ is given.

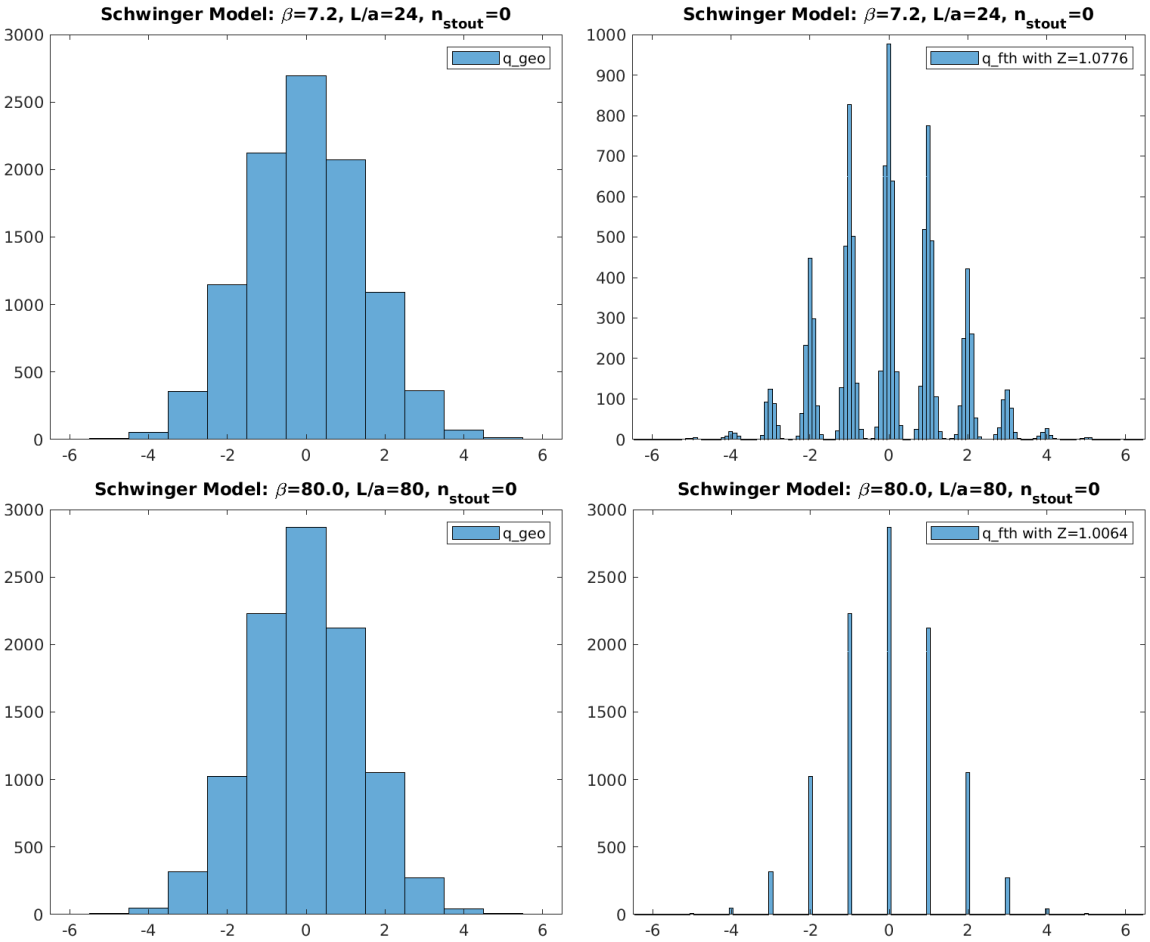

Fig. 2: Distribution of the integer valued topological charge q_{geo} (left) and of the real valued charge q_{fth} ahead of the cast-to-integer operation (right) with $n_{\text{stout}} = 0$ at $\beta = 7.2$ (top) and $\beta = 80.0$ (bottom).

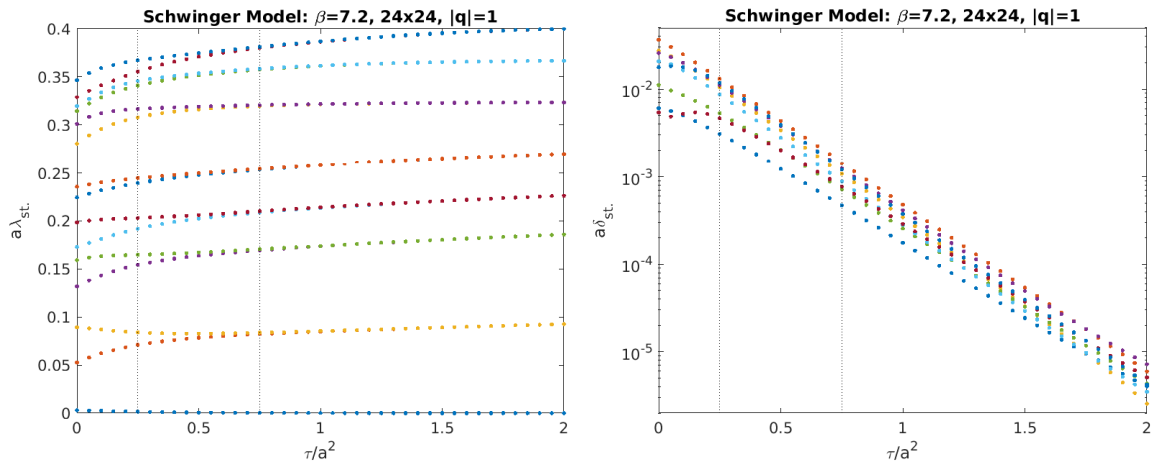

Fig. 3: Eigenvalues $a\lambda_i$ $(i = 1, \ldots, 15)$ of $D_{\rm S}$ on a $|q| = 1$ configuration at $(\beta, L/a) = (7.2, 24)$ versus the gradient flow time τ/a^2 (left) and the resulting splittings $a\delta_1 = 2a\lambda_1, a\delta_2 = a\lambda_3 - a\lambda_2, \ldots$ versus τ/a^2.

4. Taste splittings: evolution under gradient flow

In the main investigation we shall use 0, 1 and 3 steps of stout smearing [13] at $\rho = 0.25$. Still, to get an idea of the effect that any kind of smearing/smoothing/cooling of the gauge links has on the eigenvalues of a Dirac operator, we think it is best to consider the evolution of the imaginary part of the low-lying eigenvalues as a function of the gradient flow time $\tau/a^2 \in \mathbb{R}$ [17]. The result for $D_{\rm S}$ on an arbitrarily chosen configuration at $\beta = 7.2$ is shown in the left panel of Fig. 3.

In order to understand the resulting pattern, one must keep in mind that the background has $|q| = 1$. Hence one expects a pairing $\lambda_1 \leftrightarrow -\lambda_1$ (the latter one is negative and thus not shown in Fig. 3), while the subsequent pairings are $\lambda_2 \leftrightarrow \lambda_3$ and so on. Interestingly, for $\tau/a^2 = 0$ (on the left axis) it seems impossible to guess these pairings from the spacing of the eigenvalues.

However, as the smoothing evolves the pairings become gradually visible, and the splittings of the non-topological modes $\delta_2 = \lambda_3 - \lambda_2, \delta_3 = \lambda_5 - \lambda_4, \ldots$ diminish at the same more-or-less exponential rate as the would-be zero mode splitting (δ_1 on this configuration) with τ/a^2 (right panel of Fig. 3). The 1 and 3 stout smearings in the main investigation correspond to $\tau/a^2 = 0.25$ and $\tau/a^2 = 0.75$ (marked with dotted vertical lines), up to flow-time discretization effects [17].

5. Taste splittings: eigenvalue pairs after 0, 1 and 3 stout smearings

We are now in a position to look at the splittings of the three operators $D = D_{\rm S}, D_{\rm KW}, D_{\rm BC}$ on the ensembles listed, for any of the smearing levels $n_{\rm stout} = 0, 1, 3$. As mentioned before, the analysis proceeds with a view on the global topological charge of the background, since the first $|q|$ eigenvalues are paired with their negatives, while the higher eigenvalues are paired with an adjacent one. In this sense the analysis treats the $|q|$ would-be zero modes (on the positive side of the imaginary parts) different from the remaining non-topological modes.

A typical result for $n_{\rm stout} = 1$ is shown in Fig. 4. Considering the would-be zero modes, the KW splittings seem to beat the staggered splittings (columns 1,2,3 in the right panels). Regarding non-topological modes, staggered fermions seem to have the smallest intra-taste splittings, followed

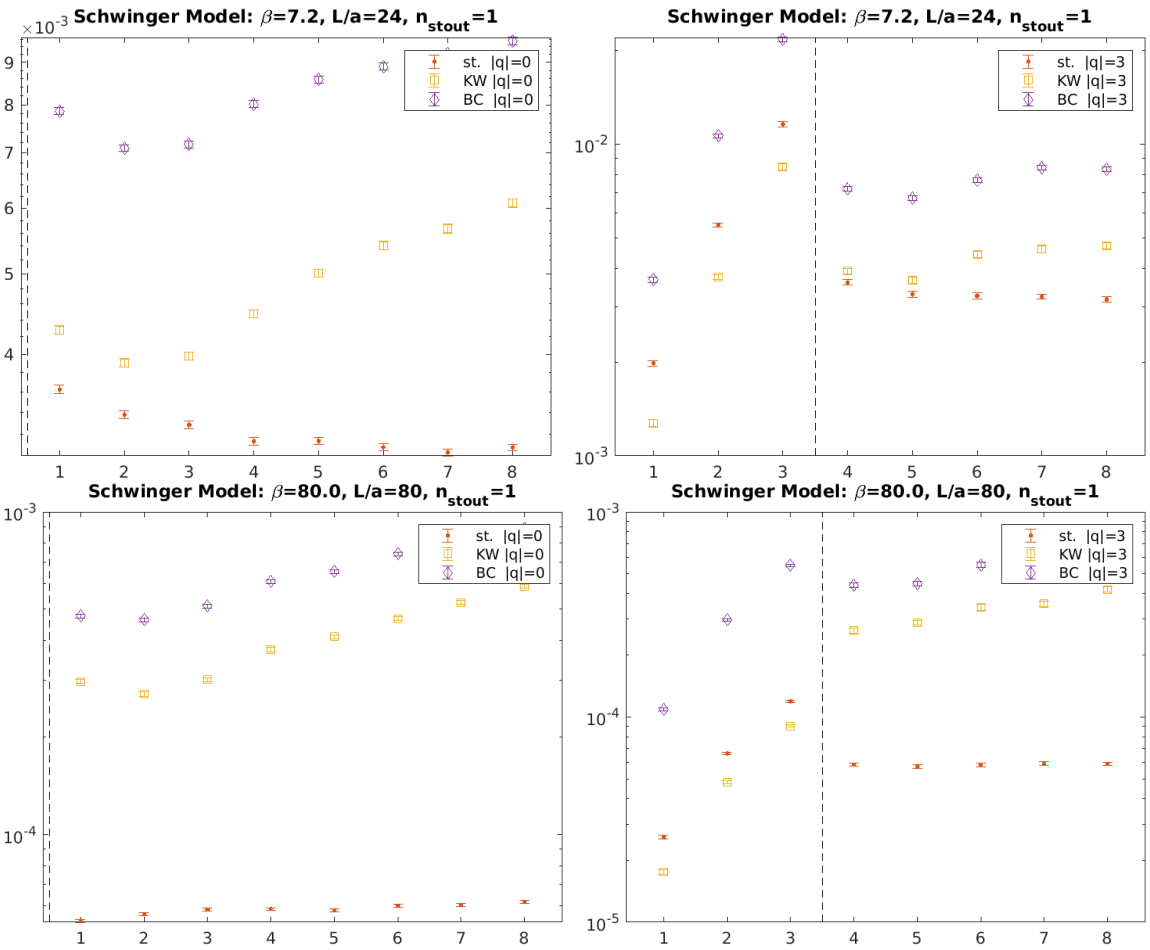

Fig. 4: Taste-splittings $a\delta_i$ ($i = 1, \ldots, 8$) of the operators $D_{\rm S}$, $D_{\rm KW}$ and $D_{\rm BC}$ at $\beta = 7.2$ (top) and $\beta = 80.0$ (bottom) for $n_{\rm stout} = 1$. The would-be zero mode splittings $a\delta_1, \ldots, a\delta_{|q|}$ are separated from the non-topological splittings $a\delta_{|q|+1}, \ldots$ by a dashed vertical line for $|q| = 0$ (left) and $|q| = 3$ (right).

by KW fermions, while BC fermions fare worst (all panels). This is for $n_{\rm stout} = 1$, and we have data for $n_{\rm stout} = 0$ and $n_{\rm stout} = 3$, too. The main effect of an increased β is that the overall scale (y-axis) becomes smaller. We also check that our data at $(L/a)^2/\beta = 80$ have only mild finite size effects.

6. Taste splittings: Symanzik scaling after 0, 1 and 3 stout smearings

With the data of the previous section in hand we can check whether the eigenvalue splittings satisfy any kind of Symanzik scaling. The standard lore says that the remnant chiral symmetry of $D_{\rm S}, D_{\rm KW}, D_{\rm BC}$ enforces cut-off effects to scale *asymptotically* like $\propto a^2$. One needs to specify whether this statement is meant to hold for the dimensionful splittings δ_i or the dimensionless $a\delta_i$.

How the first would-be zero mode splitting $a\delta_1$ depends on $a \propto \beta^{-1/2}$ is shown in Fig. 5 for two options of $|q|$ and $n_{\rm stout}$. The log-log representation suggests that (for each action) the Symanzik law is $a\delta \propto a^2$ without smearing and likely $a\delta \propto a^3$ with smearing. This is rather surprising – the standard lore says that an ultralocal modification (e.g. link smearing) of the action leaves the Symanzik universality class unchanged. With smearing we see large logarithmic corrections.

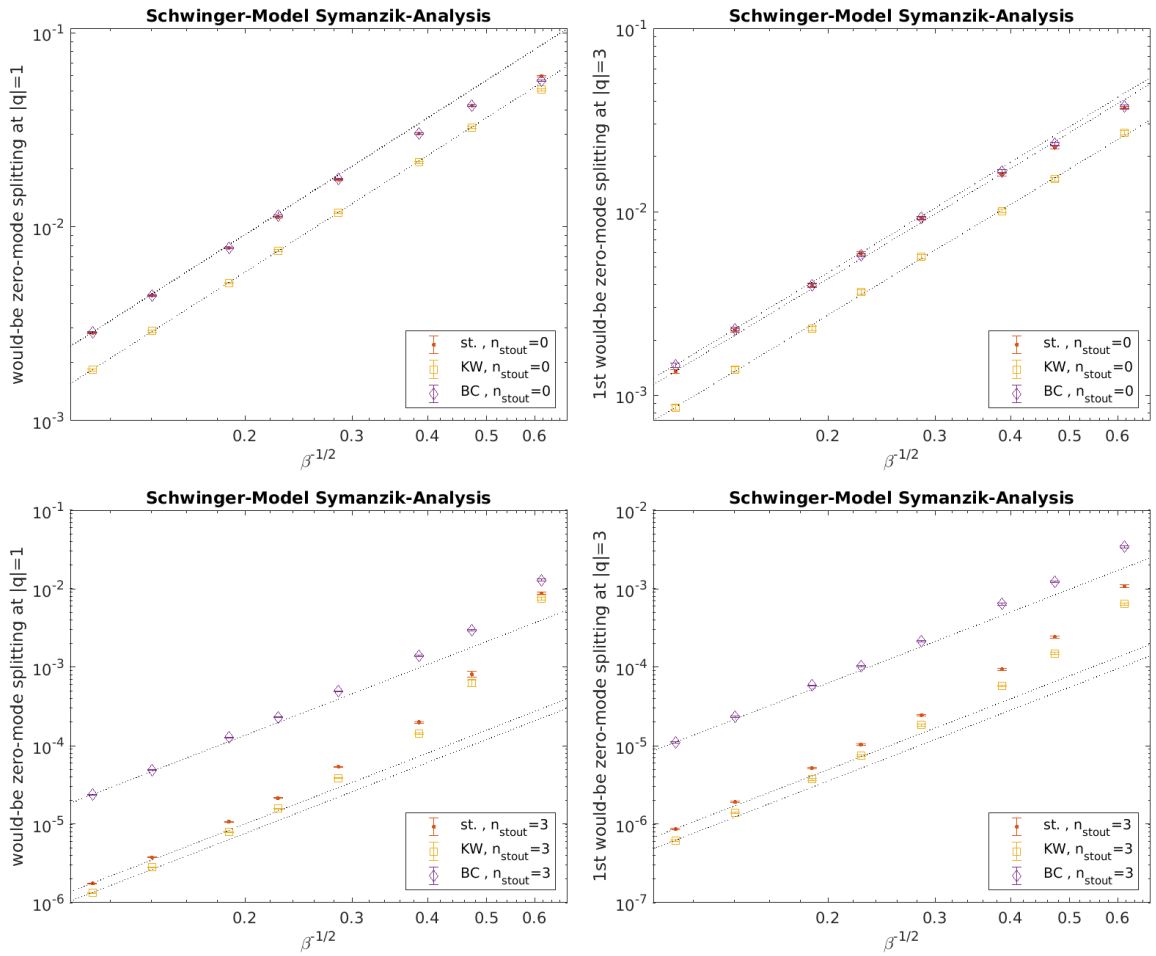

Fig. 5: Would-be zero mode splitting $a\delta_1$ versus a at $|q| = 1, 3$ (left, right) for $n_{\text{stout}} = 0, 3$ (top, bottom). The dotted lines are no fits but power laws $a\delta \propto a^2$ at $n_{\text{stout}} = 0$ (top row) and $a\delta \propto a^3$ at $n_{\text{stout}} \geq 1$ (bottom row) with a prefactor which makes them pass through the leftmost datapoint.

How the first non-topological splitting $a\delta_{|q|+1}$ depends on $a \propto \beta^{-1/2}$ is shown in Fig. 6 for two options of $|q|$ and n_{stout}. This time the situation is more diverse. For $D_{\text{KW}}, D_{\text{BC}}$ the Symanzik law is $a\delta \propto a^2$ for any n_{stout}. For D_{S} the Symanzik law is $a\delta \propto a^2$ at $n_{\text{stout}} = 0$, while the situation is less clear at $n_{\text{stout}} \geq 1$. With three stout steps the splittings pertinent to non-topological modes of D_{S} are reluctant to follow any integer-valued power law (in Fig. 6 the slope $a\delta \propto a^3$ is too steep in the range shown, but it might be appropriate for $a \to 0$). Influenced by the clear pattern without smearing (upper panels) and analogous data with gradient flow [18], one might conjecture that also the non-topological staggered splittings eventually adopt the Symanzik law $a\delta_{|q|+1} \propto a^2$. In the event this conjecture is true, it will take much finer lattices to underpin it with numerical data.

Overall, these findings are puzzling. For the splittings pertinent to would-be zero modes there seems to be a difference between the scaling law $\delta_i \propto a$ without and $\delta_i \propto a^2$ with smearing. This holds for $D = D_{\text{S}}, D_{\text{KW}}, D_{\text{BC}}$ alike. For the taste splittings of non-topological modes we find $\delta_i \propto a$ as far as we can establish a power law, regardless of the smearing level and the action chosen.

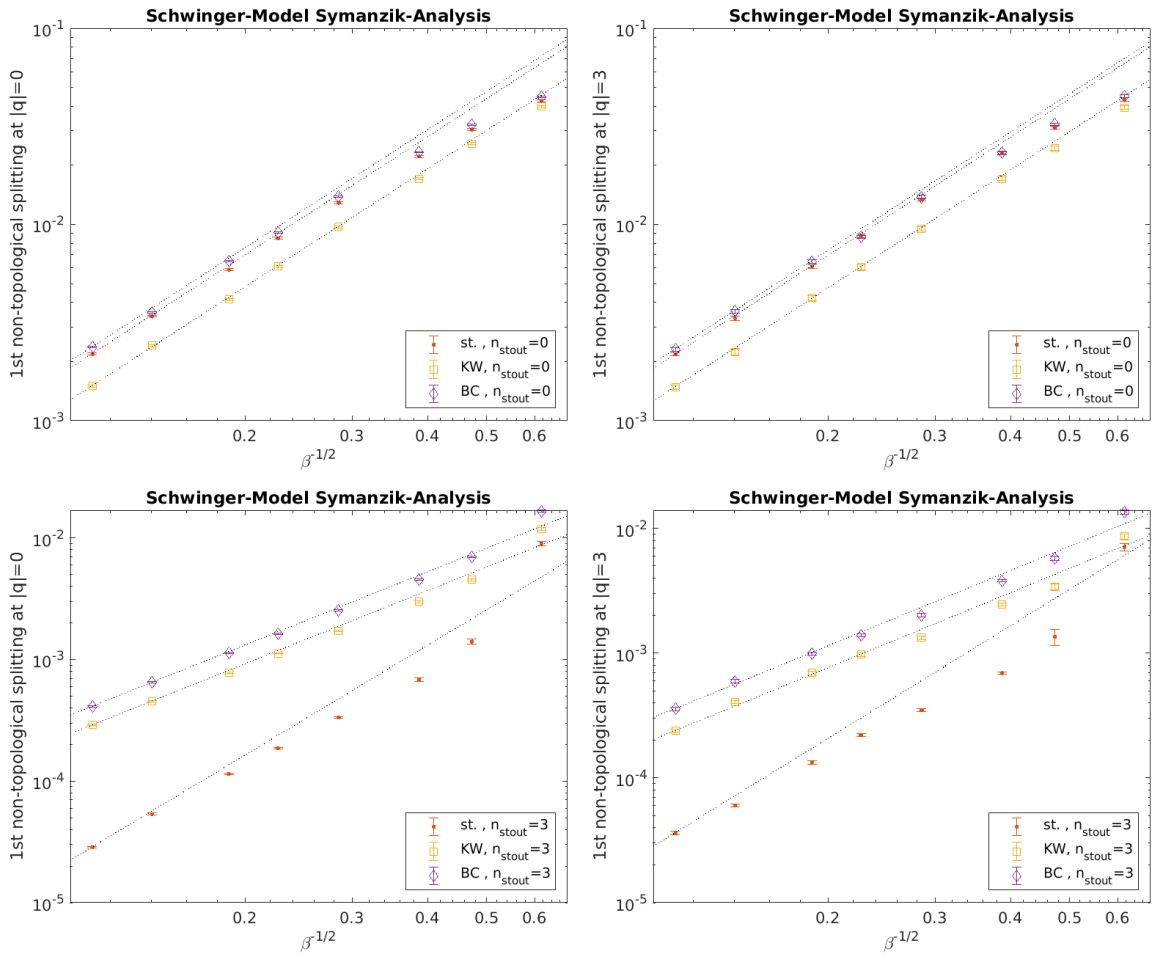

Fig. 6: First non-topological splitting $a\delta_i$ versus a at $|q| = 0, 3$ (left, right) for $n_{\text{stout}} = 0, 3$ (top, bottom). For $D_{\text{KW}}, D_{\text{BC}}$ the dotted lines are power laws $a\delta \propto a^2$, adjusted to the leftmost datapoint, at any n_{stout}. For D_{S} the data suggest $a\delta \propto a^2$ at $n_{\text{stout}} = 0$ (top) and an unclear situation at $n_{\text{stout}} \geq 1$ (bottom).

7. Summary

We investigate the intra-taste splittings of three fermion formulations (staggered, KW and BC) in the quenched Schwinger model. In 2D all three formulations are doubled, and this is why the eigenvalues come in pairs (at intermediate β the latter are visible with smearing only, cf. Fig. 3). We analyze the eigenvalue splittings with a view on the topological charge $q \in \mathbb{Z}$ of the gauge background, treating would-be zero modes and non-topological modes separately.

Our results suggest an asymptotic Symanzik scaling of the form $\delta \propto a$ for all unsmeared formulations and mode types. On the other hand, with link smearing, there is a difference between would-be zero modes and non-topological modes. For smeared KW and BC fermions we find $\delta \propto a^2$ for the former modes and $\delta \propto a$ for the latter ones. For smeared staggered fermions we find $\delta \propto a^2$ for would-be zero modes and an inconclusive behavior for non-topological modes.

Our findings are unexpected, as they challenge the view that a fixed number of stout steps (or a fixed flow-time in lattice units) leaves the Symanzik universality class unaffected. It would be interesting to complement our data with a scaling study of taste breakings based on meson mass

	$n_{\rm stout} = 0$		$n_{\rm stout} = 1, 3$	
	wbz	ntm	wbz	ntm
$\delta_{\rm stag} \propto a^p$	1	1	2	—
$\delta_{\rm KW} \propto a^p$	1	1	2	1
$\delta_{\rm BC} \propto a^p$	1	1	2	1

Tab. 3: Suggested p in the asymptotic Symanzik law $\delta \propto a^p$ for stagggered, KW and BC fermions, without and with link smearing, and for would-be zero modes ("wbz") versus non-topological modes ("ntm").

splittings (in the spirit of the checks discussed in Ref. [8]), but this requires more computer time. And of course it would be interesting to repeat this study in 4D (which again requires more computer time, and will likely result in a final precision which cannot match the precision attainable in 2D). For the time being we cannot resolve the conundrum.

References

[1] K. G. Wilson, Phys. Rev. D **10**, 2445 (1974).

[2] L. H. Karsten and J. Smit, Nucl. Phys. B **183**, 103 (1981).

[3] L. Susskind, Phys. Rev. D **16**, 3031 (1977).

[4] L. H. Karsten, Phys. Lett. **104B**, 315 (1981).

[5] F. Wilczek, Phys. Rev. Lett. **59**, 2397 (1987).

[6] M. Creutz, JHEP **0804**, 017 (2008) [arXiv:0712.1201 [hep-lat]].

[7] A. Boriçi, Phys. Rev. D **78**, 074504 (2008) [arXiv:0712.4401 [hep-lat]].

[8] A. Bazavov *et al.* [MILC], Phys. Rev. D **87**, 054505 (2013) [arXiv:1212.4768 [hep-lat]].

[9] J. S. Schwinger, Phys. Rev. **128**, 2425-2429 (1962)

[10] J. H. Lowenstein and J. A. Swieca, Annals Phys. **68**, 172-195 (1971).

[11] E. Follana *et al.* [HPQCD and UKQCD], Phys. Rev. Lett. **93**, 241601 (2004) [hep-lat/0406010].

[12] S. Durr, C. Hoelbling and U. Wenger, Phys. Rev. D **70**, 094502 (2004) [arXiv:hep-lat/0406027].

[13] C. Morningstar and M. J. Peardon, Phys. Rev. D **69**, 054501 (2004) [arXiv:hep-lat/0311018].

[14] J. Smit and J. C. Vink, Nucl. Phys. B **303**, 36-56 (1988)

[15] S. Durr, Phys. Rev. D **85**, 114503 (2012) [arXiv:1203.2560 [hep-lat]].

[16] S. Elser, [arXiv:hep-lat/0103035 [hep-lat]].

[17] M. Lüscher, JHEP **08**, 071 (2010) [err: JHEP **03**, 092 (2014)] [arXiv:1006.4518 [hep-lat]].

[18] M. Ammer and S. Durr, forthcoming